

SLAC-PUB-11542

October 2005

Advances in Light-Front Quantization and New Perspectives for QCD from AdS/CFT*

Stanley J. Brodsky

Stanford Linear Accelerator Center, Stanford University

Stanford, California 94309

sjbth@slac.stanford.edu

and

Guy F. de Téramond

Universidad de Costa Rica

San José, Costa Rica

gdt@asterix.crnet.cr

Invited talk presented at the workshop on
Light-Cone QCD and Nonperturbative Hadron Physics 2005 (LC2005)
Cairns, Australia
7–15 July, 2005

*Work supported in part by the Department of Energy under contract number DE-AC02-76SF00515.

Advances in Light-Front Quantization and New Perspectives for QCD from AdS/CFT

S. J. Brodsky^a
Guy F. de Téramond^b

^aStanford Linear Accelerator Center
Stanford University, Stanford, California 94309

^bUniversidad de Costa Rica, San José, Costa Rica

The light-front quantization of gauge theories in light-cone gauge provides a frame-independent wavefunction representation of relativistic bound states, simple forms for current matrix elements, explicit unitarity, and a Fock space built on a trivial vacuum. The AdS/CFT correspondence has led to important insights into the properties of quantum chromodynamics even though QCD is a broken conformal theory. We have recently shown how a model based on a truncated AdS space can be used to obtain the hadronic spectrum of $q\bar{q}$, qqq and gg bound states, as well as their respective light-front wavefunctions. Specific hadrons are identified by the correspondence of string modes with the dimension of the interpolating operator of the hadron's valence Fock state, including orbital angular momentum excitations. The predicted mass spectrum is linear $M \propto L$ at high orbital angular momentum, in contrast to the quadratic dependence $M^2 \propto L$ found in the description of spinning strings. Since only one parameter, the QCD scale Λ_{QCD} , is introduced, the agreement with the pattern of physical states is remarkable. In particular, the ratio of Δ to nucleon trajectories is determined by the ratio of zeros of Bessel functions. As a specific application of QCD dynamics from AdS/CFT duality, we describe a computation of the proton magnetic form factor in both the space-like and time-like regions. The extended AdS/CFT space-time theory also provides an analytic model for hadronic light-front wavefunctions, thus providing a relativistic description of hadrons in QCD at the amplitude level. The model wavefunctions display confinement at large inter-quark separation and conformal symmetry at short distances. In particular, the scaling and conformal properties of the LFWFs at high relative momenta agree with perturbative QCD. These AdS/CFT model wavefunctions could be used as an initial ansatz for a variational treatment of the light-front QCD Hamiltonian.

1. Introduction

One of the important advantage of light-front quantization is the ability to describe the structure and dynamics of hadrons at the amplitude level, Fock state by Fock state. The light-front Fock expansion provides a physical, relativistic, frame-independent description of hadrons as composites of quarks and gluons analogous to the $\psi(\vec{p})$ momentum-space wavefunction description of nonrelativistic bound states of the Schrödinger theory. Although the vacuum is formally trivial; i.e., it is an eigenstate of the free light-front Hamiltonian, the possibility of zero modes (fields with $k^+ = 0$) allows one to describe spontaneous symmetry breaking such as the Higgs mechanism of the Standard Model [1].

The light-front Fock expansion follows from the quantization of QCD at fixed light-front time $x^+ = x^0 + x^3$. The bound-state hadronic solutions $|\Psi_H\rangle$ are eigenstates of the light-front Heisenberg equation $H_{LF} |\Psi_H\rangle = M_H^2 |\Psi_H\rangle$ [2]. The spectrum of QCD is given by the eigenvalues M_H^2 . The projection of each hadronic eigensolution on the free Fock basis: $\langle n | \Psi_H \rangle \equiv \psi_{n/H}(x_i, \vec{k}_{\perp i}, \lambda_i)$ then defines the LF Fock expansion in terms of the quark and transversely polarized gluon constituents in $A^+ = 0$ light-cone gauge. The light-front wavefunctions $\psi_{n/H}(x_i, \vec{k}_{\perp i}, \lambda_i)$ are functions of the constituent light-cone fractions $x_i = k_i^+ / P^+ = (k^0 + k^z)_i / P^+$, relative transverse momenta $\vec{k}_{\perp i}$, and spin projections $S_i^z = \lambda_i$. They are relativistic and frame-independent, describing all particle number excitations n of the hadrons

The expansion has only transversely polarized gluons. The freedom to choose the light-like quantization four-vector provides an explicitly covariant formulation of light-front quantization and can be used to determine the analytic structure of light-front wave functions and to define a kinematical definition of angular momentum [3]. The front form thus provides a consistent definition of relative orbital angular momentum and J^z conservation: the total spin projection $J^z = \sum_{i=1}^n S_i^z + \sum_i^{n-1} L_i^z$ is conserved in each Fock state. The cluster decomposition theorem [4] and the vanishing of the “anomalous gravitomagnetic moment” $B(0)$ [5] are immediate properties of the LF Fock wavefunctions [6].

In principle, one can solve for the LFWFs directly from the fundamental theory using methods such as discretized light-front quantization (DLCQ) [7], the transverse lattice [8–10], lattice gauge theory moments [11], Dyson-Schwinger techniques [12], and Bethe–Salpeter techniques [3]. DLCQ has been remarkably successful in determining the entire spectrum and corresponding LFWFs in one space-one time field theories [13], including QCD(1+1) [14] and supersymmetric QCD(1+1) [15]. The DLCQ boundary conditions allow a truncation of the Fock space to finite dimensions while retaining the kinematic boost and Lorentz invariance of light-front quantization. There are also light-front solutions for Yukawa theory in physical (3+1) space-time dimensions [16,17] with a limited Fock space. As emphasized by Weinstein and Vary, new effective operator methods [18,19] which have been developed for Hamiltonian theories in condensed matter and nuclear physics, could also be applied advantageously to light-front Hamiltonian. A review of nonperturbative light-front methods may be found in Ref. [20].

As we shall discuss below, one can use the correspondence between theories defined in anti-de Sitter space and conformal field theories in 3+1 dimensions to obtain a remarkably simple but compelling phenomenological model of QCD. In particular, the AdS/CFT holographic model with a truncated warped space provides an explicit analytic form for the valence (lowest Fock state) light-front wavefunctions of hadrons with zero

mass quarks but arbitrary internal orbital angular momentum. The predicted wavefunctions display confinement at large inter-quark separation and conformal symmetry at short distances. In particular, the scaling and conformal properties of the LFWFs at high relative momenta agree with perturbative QCD. These AdS/CFT model wavefunctions could be used as an initial ansatz for a variational treatment of the full light-front QCD Hamiltonian.

2. Phenomenology of Light-Front Wavefunctions

Given the light-front wavefunctions $\psi_{n/H}(x_i, \vec{k}_{\perp i}, \lambda_i)$, one can compute a large range of hadron observables. For example, the valence and sea quark and gluon distributions which are measured in deep inelastic lepton scattering are defined from the squares of the LFWFs summed over all Fock states n . Form factors, exclusive weak transition amplitudes [21] such as $B \rightarrow \ell\nu\pi$, and the generalized parton distributions [22] measured in deeply virtual Compton scattering are (assuming the “handbag” approximation) overlaps of the initial and final LFWFs with $n = n'$ and $n = n' + 2$. The gauge-invariant distribution amplitude $\phi_H(x_i, Q)$ defined from the integral over the transverse momenta $\vec{k}_{\perp i}^2 \leq Q^2$ of the valence (smallest n) Fock state provides a fundamental measure of the hadron at the amplitude level [23,24]; they are the nonperturbative input to the factorized form of hard exclusive amplitudes and exclusive heavy hadron decays in perturbative QCD. The resulting distributions obey the DGLAP and ERBL evolution equations as a function of the maximal invariant mass, thus providing a physical factorization scheme [25]. In each case, the derived quantities satisfy the appropriate operator product expansions, sum rules, and evolution equations. However, at large x where the struck quark is far-off shell, DGLAP evolution is quenched [26], so that the fall-off of the DIS cross sections in Q^2 satisfies inclusive-exclusive duality at fixed W^2 .

The light-front Fock-state wavefunctions of hadrons in QCD display novel features, such as intrinsic gluons, asymmetric sea-quark distribu-

tions $\bar{u}(x) \neq \bar{d}(x)$, $\bar{s}(x) \neq s(x)$, and intrinsic heavy-quark Fock states [27]. Intrinsic charm and bottom quarks appear at large x in the light-front wavefunctions since this minimizes the invariant mass and off-shellness of the higher Fock state. One can use the operator product expansion to show that the probability of such states scales as $1/M_Q^2$ in contrast to $1/M_\ell^4$ fall-off of abelian theory [28]. The remarkable observations of the SELEX experiment of the double-charm baryon Ξ_{ccd} in $pA \rightarrow \Xi_{ccd}X$ and $\Sigma^- A \rightarrow \Xi_{ccd}X$ at large x_F [29] provides compelling evidence for double-charm intrinsic Fock states in the proton. The coherence of multi-particle correlations within the Fock states leads to higher-twist bosonic processes such as $e(qq) \rightarrow e'(qq)'$; although suppressed by inverse powers of Q^2 , such subprocesses are important in the duality regime of fixed W^2 , particularly in σ_L [30]. In the case of nuclei, one must include non-nucleonic “hidden color” [31] degrees of freedom of the deuteron LFWF.

2.1. Measurements of the LFWFs

The E791 experiments at Fermilab [32,33] has shown how one can measure the valence LFWF directly from the diffractive di-jet dissociation of a high energy pion $\pi A \rightarrow q\bar{q}A'$ into two jets, nearly balancing in transverse momentum, leaving the nucleus intact. The measured pion distribution in x and $(1-x)$ is similar to the form of the asymptotic distribution amplitude and the AdS/CFT prediction discussed below. The E791 experiment also find that the nuclear amplitude is additive in the number of nucleons when the quark jets are produced at high k_\perp , thus giving a dramatic confirmation of “color transparency”, a fundamental manifestation of the gauge nature of QCD [34,35].

2.2. Effects of Final State Interactions

The phase structure of hadron matrix elements is an essential feature of hadron dynamics. Although the LFWFs are real for a stable hadron, they acquire phases from initial state and final state interactions. In addition, the violation of CP invariance leads to a specific phase structure of the LFWFs.

Contrary to parton model expectations, the

rescattering of the quarks in the final state in DIS has important phenomenological consequences, such as leading-twist diffractive DIS [36] and the Sivvers single-spin asymmetry [37]. The Sivvers asymmetry depends on the same matrix elements which produce the anomalous magnetic moment of the target nucleon as well as the phase difference of the final-state interactions in different partial waves. The rescattering of the struck parton generates dominantly imaginary diffractive amplitudes, giving rise to an effective “hard pomeron” exchange and a rapidity gap between the target and diffractive system, while leaving the target intact. This Bjorken-scaling physics, which is associated with the Wilson line connecting the currents in the virtual Compton amplitude survives even in light-cone gauge. Thus there are contributions to the DIS structure functions which are not included in the light-front wave functions computed in isolation and cannot be interpreted as parton probabilities [36]. Diffractive deep inelastic scattering in turn leads to nuclear shadowing at leading twist as a result of the destructive interference of multi-step processes within the nucleus. In addition, multi-step processes involving Reggeon exchange leads to antishadowing. In fact, because Reggeon couplings are flavor specific, antishadowing is predicted to be non-universal, depending on the type of current and even the polarization of the probes in nuclear DIS [38].

Another interesting consequence of QCD at the amplitude level is the Q^2 -independent “ $J = 0$ fixed-pole” contribution $M(\gamma^*p \rightarrow \gamma p) \sim s^0 F(t)$ to the real part of the Compton amplitude, reflecting the effective contact interaction of the transverse currents [39]. Deeply virtual Compton scattering can also be studied in the time-like domain from $e^+e^- \rightarrow H^+H^-\gamma$; the lepton charge asymmetry and single-spin asymmetries allow measurements of the relative phase of time-like form factors and the $\gamma^* \rightarrow H^+H^-\gamma$ amplitude.

3. AdS/CFT Predictions for Hadron Spectra and Wavefunctions

The AdS/CFT correspondence [40], between strongly-coupled conformal gauge theory and weakly-coupled string theory in the 10-dimensional $AdS_5 \times S^5$ space is now providing a remarkable new insight into the hadron wavefunctions of QCD. The central mathematical principle underlying AdS/CFT duality is the fact that the group $SO(2,4)$ of Poincaré and conformal transformations of physical 3+1 space-time has an elegant mathematical representation on AdS_5 space where the fifth dimension has the anti-de Sitter warped metric. The group of conformal transformations $SO(2,4)$ in 3+1 space is isomorphic to the group of isometries of AdS space, $x^\mu \rightarrow \lambda x^\mu$, $r \rightarrow r/\lambda$, where r represents the coordinate in the fifth dimension. The dynamics at $x^2 \rightarrow 0$ in 3+1 space thus matches the behavior of the theory at the boundary $r \rightarrow \infty$. This allows one to map the physics of quantum field theories with conformal symmetry to an equivalent description in which scale transformations have an explicit representation in AdS space.

Even though quantum chromodynamics is a broken conformal theory, the AdS/CFT correspondence has led to important insights into the properties of QCD. For example, as shown by Polchinski and Strassler [41], the AdS/CFT duality, modified to give a mass scale, provides a non-perturbative derivation of the empirically successful dimensional counting rules [42,43] for the leading power-law fall-off of the hard exclusive scattering amplitudes of the bound states of the gauge theory. The modified theory generates the hard behavior expected from QCD instead of the soft behavior characteristic of strings. Other important applications include the description of space-like hadron form factors at large transverse momentum [44] and deep inelastic scattering structure functions at small x [45]. The power falloff of hadronic light-front wave functions (LFWF) including states with nonzero orbital angular momentum is also predicted [46].

In the original formulation by Maldacena [40], a correspondence was established between a supergravity string theory on a curved background

and a conformally invariant $\mathcal{N} = 4$ super Yang-Mills theory in four-dimensional space-time. The higher dimensional theory is $AdS_5 \times S^5$ where $R = (4\pi g_s N_C)^{1/4} \alpha_s'^{1/2}$ is the radius of AdS and the radius of the five-sphere and $\alpha_s'^{1/2}$ is the string scale. The extra dimensions of the five-dimensional sphere S^5 correspond to the $SU(4) \sim SO(6)$ global symmetry which rotates the particles present in the supersymmetric Yang Mills supermultiplet in the adjoint representation of $SU(N_C)$. In our application to QCD, baryon number in QCD is represented as a Casimir constant on S^5 .

The reason why AdS/CFT duality can have at least approximate applicability to physical QCD is based on the fact that the underlying classical QCD Lagrangian with massless quarks is scale-invariant [47]. One can thus take conformal symmetry as an initial approximation to QCD, and then systematically correct for its nonzero β function and quark masses [48]. This “conformal template” approach underlies the Banks-Zak method [49] for expansions of QCD expressions near the conformal limit and the BLM method [50] for setting the renormalization scale in perturbative QCD applications. In the BLM method the corrections to a perturbative series from the β -function are systematically absorbed into the scale of the QCD running coupling. An important example is the “Generalized Crewther Relation” [51] which relates the Bjorken and Gross-Llewellyn sum rules at the deep inelastic scale Q^2 to the e^+e^- annihilation cross sections at specific commensurate scales $s^*(Q^2) \simeq 0.52 Q^2$. The Crewther relation [52] was originally derived in conformal theory; however, after BLM scale setting, it becomes a fundamental test of physical QCD, with no uncertainties from the choice of renormalization scale or scheme.

QCD is nearly conformal at large momentum transfers where asymptotic freedom is applicable. Nevertheless, it is remarkable that dimensional scaling for exclusive processes is observed even at relatively low momentum transfer where gluon exchanges involve relatively soft momenta [53]. The observed scaling of hadron scattering at moderate momentum transfers can be understood if

the QCD coupling has an infrared fixed point [54]. In this sense, QCD resembles a strongly-coupled conformal theory.

3.1. Deriving Hadron Spectra from AdS/CFT

The duality between a gravity theory on AdS_{d+1} space and a conformal gauge theory at its d -dimensional boundary requires one to match the partition functions at the AdS boundary, $z = R^2/r \rightarrow 0$. The physical string modes $\Phi(x, r) \sim e^{-iP \cdot x} f(r)$, are plane waves along the Poincaré coordinates with four-momentum P^μ and hadronic invariant mass states $P_\mu P^\mu = \mathcal{M}^2$. For large- r or small- z , $f(r) \sim r^{-\Delta}$, where the dimension Δ of the string mode must be the same dimension as that of the interpolating operator \mathcal{O} which creates a specific hadron out of the vacuum: $\langle P | \mathcal{O} | 0 \rangle \neq 0$.

The physics of color confinement in QCD can be described in the AdS/CFT approach by truncating the AdS space to the domain $r_0 < r < \infty$, where $r_0 = \Lambda_{\text{QCD}} R^2$. The cutoff at r_0 is dual to the introduction of a mass gap Λ_{QCD} ; it breaks conformal invariance and is responsible for the generation of a spectrum of color-singlet hadronic states. The truncation of the AdS space insures that the distance between the colored quarks and gluons as they stream into the fifth dimension is limited to $z < z_0 = 1/\Lambda_{\text{QCD}}$. The resulting $3+1$ theory has both color confinement at long distances and conformal behavior at short distances. The latter property allows one to derive dimensional counting rules for form factors and other hard exclusive processes at high momentum transfer. This approach, which can be described as a “bottom-up” approach, has been successful in obtaining general properties of the low-lying hadron spectra, chiral symmetry breaking, and hadron couplings in AdS/QCD [55] in addition to the hard scattering predictions [41,45,46].

In this “classical holographic model”, the quarks and gluons propagate into the truncated AdS interior according to the AdS metric without interactions. In effect, their Wilson lines, which are represented by open strings in the fifth dimension, are rigid. The resulting equations for spin 0, $\frac{1}{2}$, 1 and $\frac{3}{2}$ hadrons on $AdS_5 \times S^5$

lead to color-singlet states with dimension 3, 4 and $\frac{9}{2}$. Consequently, only the hadronic states (dimension-3) $J^P = 0^-, 1^- q\bar{q}$ pseudoscalar and vector mesons, the (dimension- $\frac{9}{2}$) $J^P = \frac{1}{2}^+, \frac{3}{2}^+ qqq$ baryons, and the (dimension-4) $J^P = 0^+ gg$ gluonium states, can be derived in the classical holographic limit [56]. This description corresponds to the valence Fock state as represented by the light-front Fock expansion. Hadrons also fluctuate in particle number, in their color representations (such as the hidden-color states [31] of the deuteron), as well as in internal orbital angular momentum. The higher Fock components of the hadrons are manifestations of the quantum fluctuations of QCD; these correspond to the fluctuations of the bulk geometry about the fixed AdS metric. For spinning strings orbital excitations of hadronic states correspond to quantum fluctuations about the AdS metric [57]. It is thus also natural to identify higher-spin hadrons with the fluctuations around the spin 0, $\frac{1}{2}$, 1 and $\frac{3}{2}$ classical string solutions of the AdS_5 sector [56].

As a specific example, consider the twist-two (dimension minus spin) gluonium interpolating operator $\mathcal{O}_{4+L}^{\ell_1 \dots \ell_m} = F D_{\{\ell_1 \dots \ell_m\}} F$ with total internal space-time orbital momentum $L = \sum_{i=1}^m \ell_i$ and conformal dimension $\Delta_L = 4 + L$. We match the large r asymptotic behavior of each string mode to the corresponding conformal dimension of the boundary operators of each hadronic state while maintaining conformal invariance. In the conformal limit, an L quantum, which is identified with a quantum fluctuation about the AdS geometry, corresponds to an effective five-dimensional mass μ in the bulk side. The allowed values of μ are uniquely determined by requiring that asymptotically the dimensions become spaced by integers, according to the spectral relation $(\mu R)^2 = \Delta_L(\Delta_L - 4)$ [56]. The four-dimensional mass spectrum follows from the Dirichlet boundary condition $\Phi(x, z_0) = 0$, $z_0 = 1/\Lambda_{\text{QCD}}$, on the AdS string amplitudes for each wave function with spin < 2 . The eigen-spectrum is then determined from the zeros of Bessel functions, $\beta_{\alpha, k}$. The predicted spectra [56] of mesons and baryons with zero mass quarks is shown in Figs. 1 and 2. The only parameter is

$\Lambda_{\text{QCD}} = 0.263$ GeV, and 0.22 GeV for mesons and baryons, respectively.

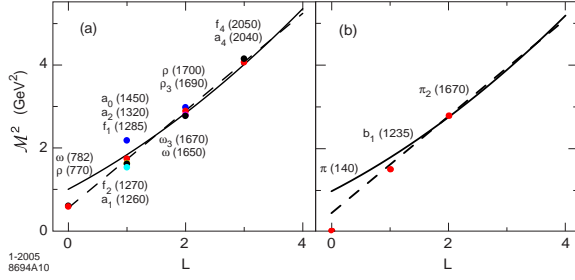


Figure 1. Light meson orbital states for $\Lambda_{\text{QCD}} = 0.263$ GeV: (a) vector mesons and (b) pseudoscalar mesons. The dashed line is a linear Regge trajectory with slope 1.16 GeV^2 .

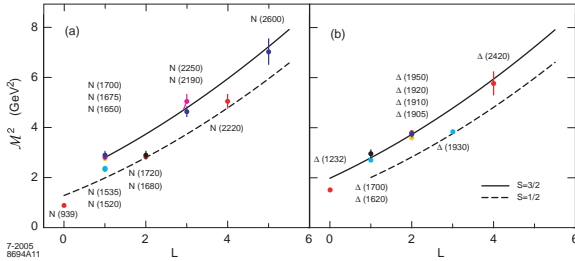


Figure 2. Light baryon orbital spectrum for $\Lambda_{\text{QCD}} = 0.22$ GeV: (a) nucleons and (b) Δ states.

3.2. Dynamics from AdS/CFT

Current matrix elements in AdS/QCD are computed from the overlap of the normalizable modes dual to the incoming and outgoing hadron Φ_I and Φ_F and the non-normalizable mode $\mathcal{A}(Q, z)$, dual to the external source [58,59]

$$F(Q^2)_{I \rightarrow F} \simeq R^{3+2\sigma} \int_0^{z_0} \frac{dz}{z^{3+2\sigma}} \Phi_F(z) \mathcal{A}(Q, z) \Phi_I(z), \quad (1)$$

where $\sigma_n = \sum_{i=1}^n \sigma_i$ is the spin of the interpolating operator \mathcal{O}_n , which creates an n -Fock state $|n\rangle$ at the AdS boundary. $\mathcal{A}(Q, z)$ has the value 1 at zero momentum transfer as the boundary limit of the external current; thus $A^\mu(x, z) = \epsilon^\mu e^{iQ \cdot x} \mathcal{A}(Q, z)$. The solution to the AdS wave equation subject to boundary conditions at $Q = 0$ and $z \rightarrow 0$ is [45] $\mathcal{A}(Q, z) = zQK_1(zQ)$, for $Q^2 \gg \Lambda_{\text{QCD}}$. At large enough $Q \sim r/R^2$, the most important contribution to the form factor comes from the region near $z \sim 1/Q$. At small z , the n -mode $\Phi^{(n)}$ scales as $\Phi^{(n)} \sim z^{\Delta_n}$, and we recover the power law scaling [42], $F(Q^2) \rightarrow [1/Q^2]^{\tau-1}$, where the twist $\tau = \Delta_n - \sigma_n$, is equal to the number of partons, $\tau_n = n$.

For $Q \sim \Lambda_{\text{QCD}}$ the simple expression for the non-normalizable mode $\mathcal{A}(Q, z)$ given above should be modified to include boundary conditions on the five-dimensional field strength, $F(x, z) = \partial A(x, z)$, at the infrared wall located at $z_0 = 1/\Lambda_{\text{QCD}}$. The external electromag-

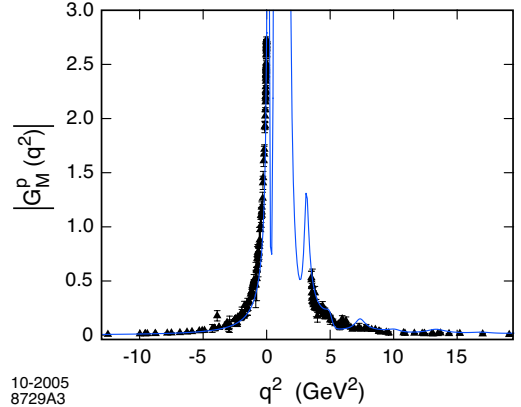


Figure 3. Space-like and time-like structure of the proton magnetic form factor in AdS/QCD for $\Lambda_{\text{QCD}} = 0.15$ GeV and $\epsilon = 40$ MeV. The space-like data are from the compilation given in Ref. [60] and the time-like data from the compilation given in [61]. The prediction in the domain $0 < q^2 < 4M_p^2$ represents an analytic continuation into the unphysical region.

netic field originates from lepton scattering and should not be confined. On the other hand, the dressed hadronic current inside the AdS cavity is coupled to quark-antiquark pairs which are confined, so it cannot propagate beyond the wall at $z = z_0$. The space-like expression for the non-normalizable mode $\mathcal{A}_{sl}(Q, z)$ satisfying the boundary conditions $F(x, z = z_0) = 0$ is

$$\mathcal{A}_{sl}(Q, z) = zQ \left[K_1(zQ) + \frac{K_0(Q/\Lambda_{\text{QCD}})}{I_0(Q/\Lambda_{\text{QCD}})} I_1(zQ) \right], \quad (2)$$

in the gauge where $A^z(x, z) = 0$. The expression for the mode dual to the external source $\mathcal{A}_{tl}(Q, z)$ in the time-like region, follows from analytic continuation $Q \rightarrow -iQ$ in $\mathcal{A}_{sl}(Q, z)$. Thus

$$\mathcal{A}_{tl}(Q, z) = \mathcal{A}_{sl}(-iQ, z) = -zQ \frac{\pi}{2} \left[Y_1(zQ) - \frac{Y_0(Q/\Lambda_{\text{QCD}})}{J_0(Q/\Lambda_{\text{QCD}})} J_1(zQ) \right]. \quad (3)$$

In the space-like region the string mode (2) is damped inside the cavity, but for time-like processes the effect from (3) is amplified. The re-

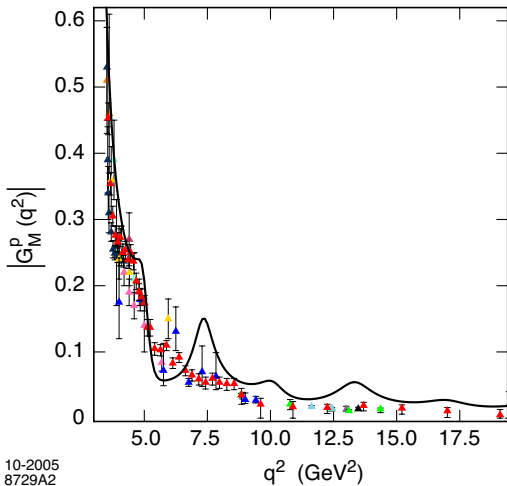


Figure 4. Time-like results for the proton magnetic form factor in AdS/QCD for $\Lambda_{\text{QCD}} = 0.15$ GeV and $\epsilon = 40$ MeV. The data are from the compilation given in Ref. [61].

sults thus become sensitive to the behavior of the \mathcal{A} near the cutoff at $z = z_0$. We introduce a small shift in Λ_{QCD} in the expression for \mathcal{A}_{tl} , $\Lambda_{\text{QCD}} \rightarrow \Lambda_{\text{QCD}} - i\epsilon$, to smear out the truncation boundary conditions in the fifth dimension, to avoid sharp cusps in the results for the time-like form factor. A numerical computation for the proton magnetic form factor in the space and time-like regions, gives the general structure shown in Fig. 3. The results correspond to a $L = 0$ proton state. It is interesting to compare the holographic predictions with a model-independent analysis of nucleon form factors using dispersion relations [60]. A more detailed comparison including recent time-like data is given in Fig. 4.

4. AdS/CFT Predictions for Light-Front Wavefunctions

The AdS/QCD correspondence provides a simple description of hadrons at the amplitude level by mapping string modes to the impact space representation of LFWFs. It is useful to define the partonic variables $x_i \vec{r}_{\perp i} = x_i \vec{R}_{\perp} + \vec{b}_{\perp i}$, where $\vec{r}_{\perp i}$ are the physical position coordinates, $\vec{b}_{\perp i}$ are frame-independent internal coordinates, $\sum_i \vec{b}_{\perp i} = 0$, and \vec{R}_{\perp} is the hadron transverse center of momentum $\vec{R}_{\perp} = \sum_i x_i \vec{r}_{\perp i}$, $\sum_i x_i = 1$. We find for a two-parton LFWF the Lorentz-invariant form

$$\tilde{\psi}_L(x, \vec{b}_{\perp}) = C x(1-x) \times \frac{J_{1+L} \left(|\vec{b}_{\perp}| \sqrt{x(1-x)} \beta_{1+L,k} \Lambda_{\text{QCD}} \right)}{|\vec{b}_{\perp}| \sqrt{x(1-x)}}. \quad (4)$$

The $\beta_{1+L,k}$ are the zeroes of the Bessel functions reflecting the Dirichlet boundary condition. The variable $\zeta = |\vec{b}_{\perp}| \sqrt{x(1-x)}$, $0 \leq \zeta \leq \Lambda_{\text{QCD}}^{-1}$, represents the invariant separation between quarks. In the case of a two-parton state, it gives a direct relation between the scale of the invariant separation between quarks, ζ , and the holographic coordinate in AdS space: $\zeta = z = R^2/r$. The ground state and first orbital eigenmode are depicted in Fig. 5. The distribution in x and $(1-x)$ measured in the E791 experiment for diffractive

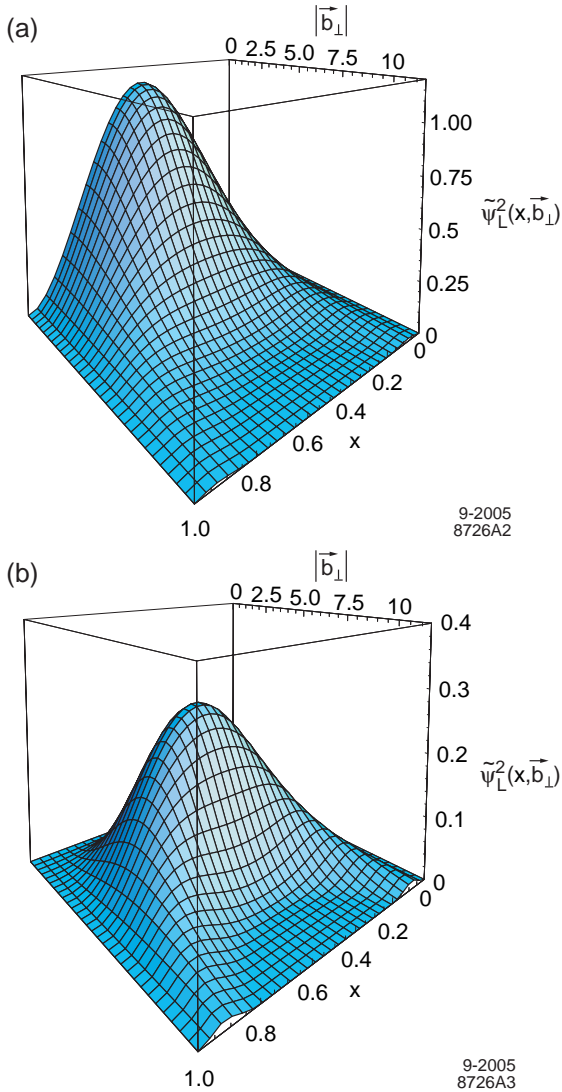


Figure 5. Prediction for the square of the two-parton bound-state light-front wave function $\tilde{\psi}_L(x, \vec{b}_\perp)$ as function of the constituents longitudinal momentum fraction x and $1-x$ and the impact space relative coordinate \vec{b}_\perp : (a) $L=0$ and (b) $L=1$.

dijet production $\pi A \rightarrow \text{Jet Jet } A$ is consistent with the AdS/CFT prediction [32,33].

5. Concluding Remarks

The holographic model is quite successful in describing the known light hadron spectrum and hadronic form factors. Since basically only one parameter, the QCD scale Λ_{QCD} , is introduced, the agreement with the pattern of masses of the physical hadronic states and the space and time-like proton form factor data is remarkable. In particular, the ratio of Δ to nucleon trajectories is determined by the ratio of zeros of Bessel functions. As we have described, non-zero orbital angular momentum and higher Fock-states require the introduction of a Casimir operator derived from quantum fluctuations. It is interesting to note that the predicted mass spectrum $M \propto L$ at high orbital angular momentum, in contrast to the quadratic dependence $M^2 \propto L$ found in traditional string theory. The only mass scale is Λ_{QCD} . Only dimension-3, $\frac{9}{2}$ and 4 states $\bar{q}q$, qqq , and gg appear in the duality at the classical level, thus explaining the suppression of $C = +$ odderon exchange.

We have also shown how one can use the extended AdS/CFT space-time theory to obtain a model for the form of hadron LFWFs. The model wavefunctions display confinement at large inter-quark separation and conformal symmetry at short distances. In particular, the scaling and conformal properties of the LFWFs at high relative momenta agree with perturbative QCD [62]. These AdS/CFT model wavefunctions could be used as an initial ansatz for a variational treatment of the light-front QCD Hamiltonian. The dominance of the quark-interchange mechanism in hard exclusive processes also emerges naturally from the classical duality of the holographic model.

Acknowledgments

Presented by SJB at the Workshop On Light-Cone QCD And Nonperturbative Hadron Physics 2005 (LC 2005), 7-15 July 2005, Cairns, Queensland, Australia. We thank Simone Pacetti and

Diego Bettoni for making available their data files for the proton form factor. This work was supported by the Department of Energy contract DE-AC02-76SF00515.

REFERENCES

1. P. P. Srivastava and S. J. Brodsky, Phys. Rev. D **66**, 045019 (2002) [arXiv:hep-ph/0202141].
2. S. J. Brodsky, H. C. Pauli and S. S. Pinsky, Phys. Rept. **301**, 299 (1998) [arXiv:hep-ph/9705477].
3. S. J. Brodsky, J. R. Hiller, D. S. Hwang and V. A. Karmanov, Phys. Rev. D **69**, 076001 (2004) [arXiv:hep-ph/0311218].
4. S. J. Brodsky and C. R. Ji, Phys. Rev. D **33**, 2653 (1986).
5. O. V. Teryaev, arXiv:hep-ph/9904376.
6. S. J. Brodsky, D. S. Hwang, B. Q. Ma and I. Schmidt, Nucl. Phys. B **593**, 311 (2001) [arXiv:hep-th/0003082].
7. H. C. Pauli and S. J. Brodsky, Phys. Rev. D **32**, 2001 (1985).
8. W. A. Bardeen, R. B. Pearson and E. Rabinovici, Phys. Rev. D **21**, 1037 (1980).
9. S. Dalley, Few Body Syst. **36**, 69 (2005) [arXiv:hep-ph/0409139].
10. M. Burkardt and S. Dalley, Prog. Part. Nucl. Phys. **48**, 317 (2002) [arXiv:hep-ph/0112007].
11. L. Del Debbio, M. Di Pierro, A. Dougall and C. T. Sachrajda [UKQCD collaboration], Nucl. Phys. Proc. Suppl. **83**, 235 (2000) [arXiv:hep-lat/9909147].
12. P. Maris and C. D. Roberts, Int. J. Mod. Phys. E **12**, 297 (2003) [arXiv:nucl-th/0301049].
13. D. J. Gross, A. Hashimoto and I. R. Klebanov, Phys. Rev. D **57**, 6420 (1998) [arXiv:hep-th/9710240].
14. K. Hornbostel, S. J. Brodsky and H. C. Pauli, Phys. Rev. D **41**, 3814 (1990).
15. M. Harada, J. R. Hiller, S. Pinsky and N. Salwen, Phys. Rev. D **70**, 045015 (2004) [arXiv:hep-th/0404123].
16. S. J. Brodsky, J. R. Hiller and G. McCartor, Annals Phys. **305**, 266 (2003) [arXiv:hep-th/0209028].
17. S. J. Brodsky, J. R. Hiller and G. McCartor, arXiv:hep-ph/0508295.
18. M. Weinstein, arXiv:hep-th/0410113.
19. H. Zhan, A. Nogga, B. R. Barrett, J. P. Vary and P. Navratil, Phys. Rev. C **69**, 034302 (2004) [arXiv:nucl-th/0401047].
20. S. J. Brodsky, Few Body Syst. **36**, 35 (2005) [arXiv:hep-ph/0411056].
21. S. J. Brodsky and D. S. Hwang, Nucl. Phys. B **543**, 239 (1999) [arXiv:hep-ph/9806358].
22. S. J. Brodsky, M. Diehl and D. S. Hwang, Nucl. Phys. B **596**, 99 (2001) [arXiv:hep-ph/0009254].
23. G. P. Lepage and S. J. Brodsky, Phys. Lett. B **87**, 359 (1979).
24. A. V. Efremov and A. V. Radyushkin, Phys. Lett. B **94**, 245 (1980).
25. G. P. Lepage and S. J. Brodsky, Phys. Rev. D **22**, 2157 (1980).
26. S. J. Brodsky and G. P. Lepage, SLAC-PUB-2294, *Presented at the Workshop on Current Topics in High Energy Physics, Cal Tech., Pasadena, Calif., Feb 13-17, 1979*.
27. S. J. Brodsky, P. Hoyer, C. Peterson and N. Sakai, Phys. Lett. B **93**, 451 (1980).
28. M. Franz, M. V. Polyakov and K. Goeke, Phys. Rev. D **62**, 074024 (2000) [arXiv:hep-ph/0002240].
29. J. Engelfried [SELEX Collaboration], Nucl. Phys. A **752**, 121 (2005).
30. S. J. Brodsky, E. L. Berger and G. P. Lepage, SLAC-PUB-3027, *Presented at the Workshop on Drell-Yan Processes, Batavia, Ill., Oct 7-8, 1982*.
31. S. J. Brodsky, C. R. Ji and G. P. Lepage, Phys. Rev. Lett. **51**, 83 (1983).
32. D. Ashery [E791 Collaboration], arXiv:hep-ex/0205011.
33. E. M. Aitala *et al.* [E791 Collaboration], Phys. Rev. Lett. **86**, 4768 (2001) [arXiv:hep-ex/0010043].
34. G. Bertsch, S. J. Brodsky, A. S. Goldhaber and J. F. Gunion, Phys. Rev. Lett. **47**, 297 (1981).
35. S. J. Brodsky and A. H. Mueller, Phys. Lett. B **206**, 685 (1988).
36. S. J. Brodsky, P. Hoyer, N. Marchal, S. Peigne and F. Sannino, Phys. Rev. D **65**, 114025 (2002) [arXiv:hep-ph/0104291].

37. S. J. Brodsky, D. S. Hwang and I. Schmidt, Phys. Lett. B **530**, 99 (2002) [arXiv:hep-ph/0201296].
38. S. J. Brodsky, I. Schmidt and J. J. Yang, Phys. Rev. D **70**, 116003 (2004) [arXiv:hep-ph/0409279].
39. S. J. Brodsky, F. E. Close and J. F. Gunion, Phys. Rev. D **5**, 1384 (1972).
40. J. M. Maldacena, Adv. Theor. Math. Phys. **2**, 231 (1998) [Int. J. Theor. Phys. **38**, 1113 (1999)] [arXiv:hep-th/9711200].
41. J. Polchinski and M. J. Strassler, Phys. Rev. Lett. **88**, 031601 (2002) [arXiv:hep-th/0109174].
42. S. J. Brodsky and G. R. Farrar, Phys. Rev. Lett. **31**, 1153 (1973).
43. V. A. Matveev, R. M. Muradian and A. N. Tavkhelidze, Lett. Nuovo Cim. **7**, 719 (1973).
44. J. Polchinski and L. Susskind, arXiv:hep-th/0112204.
45. J. Polchinski and M. J. Strassler, JHEP **0305**, 012 (2003) [arXiv:hep-th/0209211].
46. S. J. Brodsky and G. F. de Teramond, Phys. Lett. B **582**, 211 (2004) [arXiv:hep-th/0310227].
47. G. Parisi, Phys. Lett. B **39**, 643 (1972).
48. S. J. Brodsky, Y. Frishman and G. P. Lepage, Phys. Lett. B **167**, 347 (1986).
49. T. Banks and A. Zaks, Nucl. Phys. B **196**, 189 (1982).
50. S. J. Brodsky, G. P. Lepage and P. B. Mackenzie, Phys. Rev. D **28**, 228 (1983).
51. S. J. Brodsky, G. T. Gabadadze, A. L. Kataev and H. J. Lu, Phys. Lett. B **372**, 133 (1996) [arXiv:hep-ph/9512367].
52. R. J. Crewther, Phys. Rev. Lett. **28**, 1421 (1972).
53. G. F. de Teramond and S. J. Brodsky, arXiv:hep-ph/0507273.
54. S. J. Brodsky, arXiv:hep-ph/0408069.
55. H. Boschi-Filho and N. R. F. Braga, JHEP **0305**, 009 (2003) [arXiv:hep-th/0212207]; S. Hong, S. Yoon and M. J. Strassler, arXiv:hep-ph/0501197; G. F. de Teramond and S. J. Brodsky, arXiv:hep-th/0409074; J. Erlich, E. Katz, D. T. Son and M. A. Stephanov, arXiv:hep-ph/0501128; L. Da Rold and A. Pomarol, Nucl. Phys. B **721**, 79 (2005) [arXiv:hep-ph/0501218]; arXiv:hep-ph/0510268; N. Evans, J. P. Shock and T. Waterson, Phys. Lett. B **622**, 165 (2005) [arXiv:hep-th/0505250]; J. Hirn and V. Sanz, arXiv:hep-ph/0507049; H. Boschi-Filho, N. R. F. Braga and H. L. Carrion, arXiv:hep-th/0507063.
56. G. F. de Teramond and S. J. Brodsky, Phys. Rev. Lett. **94**, 201601 (2005) [arXiv:hep-th/0501022].
57. S. S. Gubser, I. R. Klebanov and A. M. Polyakov, Nucl. Phys. B **636**, 99 (2002) [arXiv:hep-th/0204051].
58. S. Hong, S. Yoon and M. J. Strassler, JHEP **0404**, 046 (2004) [arXiv:hep-th/0312071].
59. S. Hong, S. Yoon and M. J. Strassler, arXiv:hep-th/0409118.
60. R. Baldini, S. Dubnicka, P. Gauzzi, S. Pacetti, E. Pasqualucci and Y. Srivastava, Eur. Phys. J. C **11**, 709 (1999).
61. D. Bettoni, *Presented at the Workshop on Nucleon Form Factors, Frascati, Italy, Oct 12-14, 2005*.
62. X. d. Ji, J. P. Ma and F. Yuan, Phys. Rev. Lett. **90**, 241601 (2003) [arXiv:hep-ph/0301141].